

Original software publication



# DeepWealth: A generalizable open-source deep learning framework using satellite images for well-being estimation

Ali Ben Abbes<sup>a,b,\*</sup>, Jeaneth Machicao<sup>b</sup>, Pedro L.P. Corrêa<sup>b</sup>, Alison Specht<sup>c</sup>, Rodolphe Devillers<sup>d</sup>, Jean P. Ometto<sup>e</sup>, Yasuhisa Kondo<sup>f,g</sup>, David Mouillot<sup>h</sup>

<sup>a</sup> FRB-CESAB, Montpellier, France

<sup>b</sup> Escola Politécnica da Universidade de São Paulo, Brazil

<sup>c</sup> Terrestrial Ecosystem Research Network, University of Queensland, Australia

<sup>d</sup> Espace-Dev (IRD, Univ. Reunion), France

<sup>e</sup> Instituto Nacional de Pesquisas Espaciais, Brazil

<sup>f</sup> Research Institute for Humanity and Nature, Japan

<sup>g</sup> Graduate University for Advanced Studies, SOKENDAI, Japan

<sup>h</sup> MARBEC (Univ. Montpellier, CNRS, Ifremer, IRD), France

## ARTICLE INFO

### Keywords:

Deep learning  
Poverty  
SDG1  
Earth observation  
Socioeconomic indices

## ABSTRACT

Measuring socioeconomic indices at the scale of regions or countries is required in various contexts, in particular to inform public policies. The use of Deep Learning (DL) and Earth Observation (EO) data is becoming increasingly common to estimate specific variables like societal wealth. This paper presents an end-to-end framework 'DeepWealth' that calculates such a wealth index using open-source EO data and DL. We use a multidisciplinary approach incorporating satellite imagery, socio-economic data, and DL models. We demonstrate the effectiveness and generalizability of DeepWealth by training it on 24 African countries and deploying it in Madagascar, Brazil and Japan. Our results show that DeepWealth provides accurate and stable wealth index estimates with an  $R^2$  of 0.69. It empowers computer-literate users skilled in Python and R to estimate and visualize well-being-related data. This open-source framework follows FAIR (Findable, Accessible, Interoperable, Reusable) principles, providing data, source code, metadata, and training checkpoints with its source code made available on Zenodo and GitHub. In this manner, we provide a DL framework that is reproducible and replicable.

## Code metadata

Current code version	v1.0
Permanent link to code/repository used for this code version	<a href="https://github.com/ElsevierSoftwareX/SOFTX-D-24-00090">https://github.com/ElsevierSoftwareX/SOFTX-D-24-00090</a>
Permanent link to reproducible capsule	To-be prepared
Legal code license	MIT
Code versioning system used	Git
Software code languages, tools and services used	Python, R
Compilation requirements, operating environments and dependencies	CUDA, tensorflow-gpu=1.15, python=3.7, Linux
If available, link to developer documentation/manual	<a href="https://github.com/PARSECworld/DeepWealth/blob/master/README.md">https://github.com/PARSECworld/DeepWealth/blob/master/README.md</a>
Support email for questions	<a href="mailto:ali.benabbes@yahoo.fr">ali.benabbes@yahoo.fr</a>

\* Corresponding author at: FRB-CESAB, Montpellier, France.

E-mail addresses: [ali.benabbes@yahoo.fr](mailto:ali.benabbes@yahoo.fr) (Ali Ben Abbes), [machicao@usp.br](mailto:machicao@usp.br) (Jeaneth Machicao), [pedro.correa@usp.br](mailto:pedro.correa@usp.br) (Pedro L.P. Corrêa), [a.specht@uq.edu.au](mailto:a.specht@uq.edu.au) (Alison Specht), [rodolphe.devillers@ird.fr](mailto:rodolphe.devillers@ird.fr) (Rodolphe Devillers), [jean.ometto@inpe.br](mailto:jean.ometto@inpe.br) (Jean P. Ometto), [kondo@chikyu.ac.jp](mailto:kondo@chikyu.ac.jp) (Yasuhisa Kondo), [david.mouillot@umontpellier.fr](mailto:david.mouillot@umontpellier.fr) (David Mouillot).

<https://doi.org/10.1016/j.softx.2024.101785>

Received 23 March 2024; Received in revised form 27 May 2024; Accepted 4 June 2024

Available online 21 June 2024

2352-7110/© 2024 The Author(s). Published by Elsevier B.V. This is an open access article under the CC BY-NC license (<http://creativecommons.org/licenses/by-nc/4.0/>).

## 1. Motivation and significance

The increase of publicly available very high resolution Earth Observations (EO) data, together with tools that can easily access and manipulate those data, has become a key factor in supporting the achievement of the United Nations Sustainable Development Goals (SDGs) [1–3]. EO data are increasingly used in this context, providing valuable insights and information to policy-makers, researchers, and practitioners on natural and human landscapes and their evolutions. EO data can help monitor progress towards SDGs, especially those related to climate, land, oceans, and water resources, and facilitate evidence-based decision-making, which ultimately supports the implementation of sustainable development strategies at all levels [4–6]. These data are often combined with ground-truthed data to help extract information from those images. Machine Learning (ML) algorithms can for instance be used to analyze patterns and relationships in EO data to generate new datasets. By learning from the target variable and its relevant features, ML models can identify correlations that humans might miss, leading to the creation of new datasets that can enhance our understanding of the Earth's observations and assist in various applications [6–9].

Deep Learning (DL) models have recently been used to tackle classification and regression tasks across diverse domains, predicting variables with a high degree of confidence [10]. DL has proved to be highly effective, with its ability to extract nuanced features from large amounts of data. Moreover, such models establish a temporal link, making DL an invaluable tool for analyzing and interpreting dynamic changes over time. Overall, DL is poised to play a major role in shaping the future of data-driven research [11,12]. The success of DL, however, depends directly on the quantity and quality of the data used to train those algorithms. Building a trained DL model is a time-consuming task, which becomes more prolonged when the data come from several sources.

This paper focuses on the use of DL for estimating well-being in rural communities using large spatial-temporal datasets of EO data. In this way, populations' overall wealth could be assessed on a more continuous basis, rather than relying on the decadal census typically used for making such an assessment. Conducting such analyses can however be challenging as obtaining the large datasets required for DL to reach high performance can be problematic [13]. The selection of a satellite sensor that aligns with the socioeconomic survey granularity is also not easy [13], and the quality of the training process can be confounded by noise in the ground-truthing data. Building on previous DL experiments is not often possible, as their reproducibility and replicability depend on dataset quality and a good description of the DL architecture [14].

Several DL-facilitated estimations of socioeconomic conditions have been conducted with some success using satellite images [13,15,16], street view images [17]. Due to the high demand for data when using Convolutional Neural Network (CNN) methods, most studies are limited to a single time stamp.

DL models have been used for socioeconomic condition estimation in various regions across the globe, such as in Thailand and Vietnam [18], China [19], Africa [13], and in Brazil [20]. However, there are limitations in accurately capturing rural areas and ensuring data quality. This leads to a lack of necessary information for precise analysis and decision-making. By analyzing multispectral (MS) and nightlight (NL) images and combining them with data from Demographic and Health Survey surveys (DHS) data, [13] introduced a new method to assess the economic well-being of 19,669 African villages. The approach using satellite imagery and DL techniques allowed estimating the well-being indicator with a  $R^2$  of 0.70.

Such deep learning-based models that achieve promising performance have motivated researchers to construct end-to-end pipelines that mimic the architectural and representational properties of the real world [21]. The framework described in our paper was replicated from the DL model developed by [13]. The common workflow for a DL-based

multi-disciplinary method assessing socioeconomic conditions (wealth or poverty) in clusters (i.e. villages) using survey data [13,15,16,20,22] starts with gathering the relevant socioeconomic data. These datasets are preprocessed in order to prepare the data for training. After the preprocessing task is completed, the DL-based methodology is used to obtain socioeconomic estimations for an area, as presented in [14].

Here, we present DeepWealth, an open-source software that uses freely available satellite images to estimate well-being levels. The model was trained on satellite images and socioeconomic data from Africa and has been adapted to other geographic regions. The DL training stage has been performed using 24 years (1997–2020) of data, making it the longest temporal duration used in such an application. We applied the model to three case studies for technical validation. The proposed estimation model can potentially improve the accuracy and timeliness of well-being estimates for decision-makers in various fields such as global health, humanitarian aid, and economic policy.

This framework is designed in accordance with the FAIR principles [23] to ensure that our data, source code, meta-data, and training checkpoints are easily locatable, openly accessible, compatible with other datasets and tools, and well-documented. By making our resources available on platforms like Zenodo and GitHub, we support reproducibility and replicability, which are essential for advancing scientific research.

## 2. Software description

This section provides an overview of how our framework is structured and how it can be implemented in practice. We present the main components of DeepWealth, as shown in Fig. 1. The data and scripts available on the DeepWealth data repository are held in 3 folders (A, B and C): (A) 'R scripts' for generating the geographic coordinates at a scale of  $\sim 6 \times 6$  km in each study area and for building the wealth index based on available socio-economic surveys, (B) 'Python scripts' providing all notebook scripts to enable reproduction and replication of the well-being estimation pipeline, and (C) 'Checkpoints' for the trained models for both MS and NL satellites images to be used for future case studies.

### 2.1. Dataset collection

The training data used 92 household surveys from 24 African countries from 1997 to 2020. The countries were: Angola, Benin, Burkina Faso, Cameroon, Côte d'Ivoire, Democratic Republic of Congo, Ethiopia, Ghana, Guinea, Kenya, Lesotho, Malawi, Mali, Mozambique, Nigeria, Madagascar, Rwanda, Senegal, Sierra Leone, Tanzania, Togo, Uganda, Zambia, and Zimbabwe. Training data were collected in two phases. In a first phase, a wealth index was constructed using Demographic and Health Surveys (DHS) data accessed through a DHS portal request <https://dhsprogram.com/data/available-datasets.cfm> [24]. DHS data collate national household surveys and provide data on a wide range of indicators. [The DHS data for these countries was a valuable resource due to its extensive coverage of over 39 years, as well as its inclusion of geospatial information. This enabled us to estimate well-being indicators over time, providing a unique opportunity to examine trends and patterns in well-being across different regions.] The following variables were used for this study: the number of rooms occupied in a house, whether the house had electricity, the quality of flooring in the house, the water supply, and whether the house had a toilet, a telephone, a radio, a television, cars, and motorcycles. Principal component analysis (PCA) was performed in R, version 3.6, to construct a multidimensional wealth index [25,26]. The first principal component of the DHS response was taken as the wealth index. The wealth index constructed for 36,182 villages is shown in Fig. 2 and more details are in the Supplementary Material.

The wealth index values obtained from the analyses of DHS data ranged from  $-2.3$  (poorest) to  $2.5$  (richest), indicating a wide disparity in wealth levels across the villages.

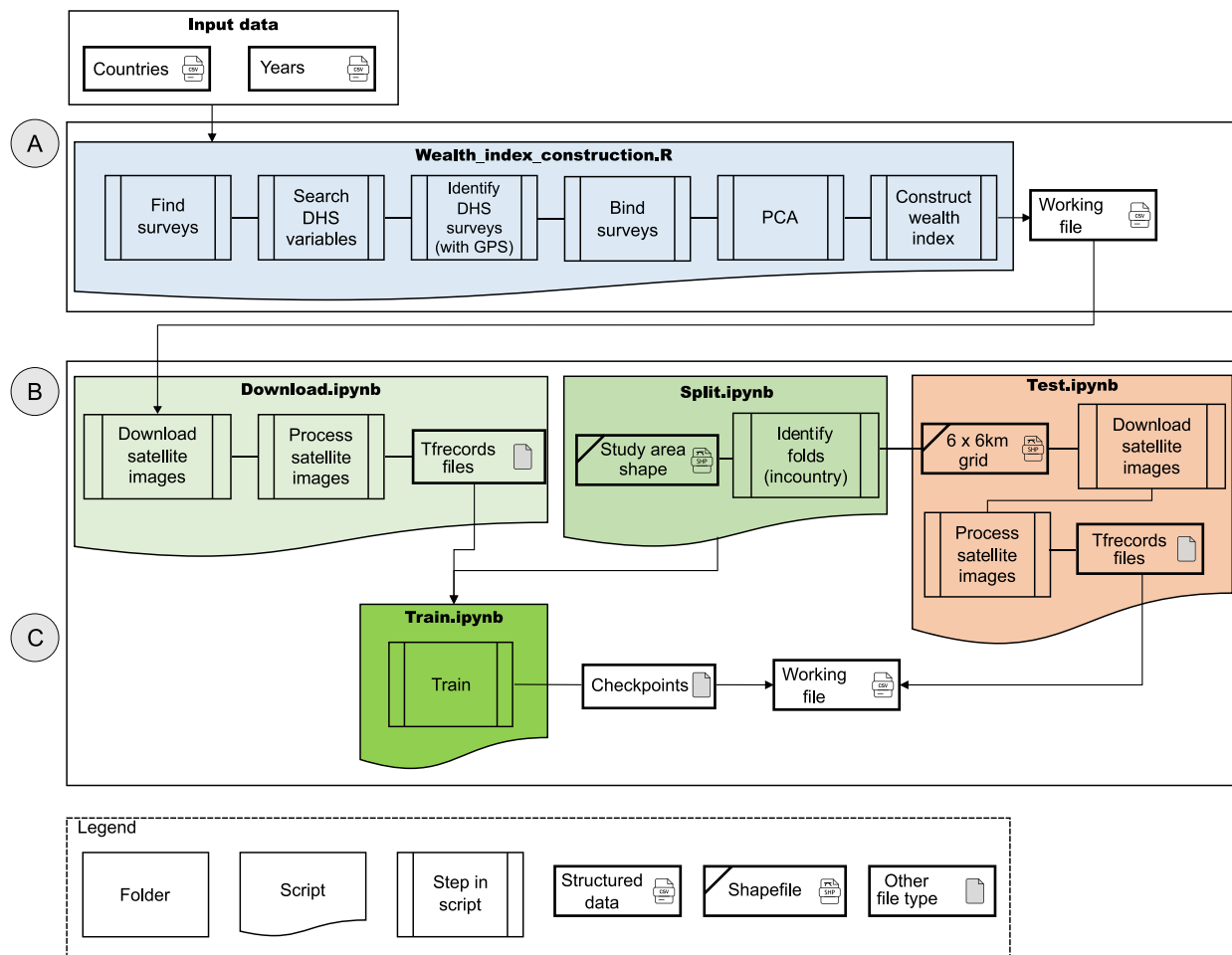


Fig. 1. Overview of DeepWealth framework and code structure organized into folders (A) 'R scripts', (B) 'Python scripts', and (C) 'Checkpoints'.

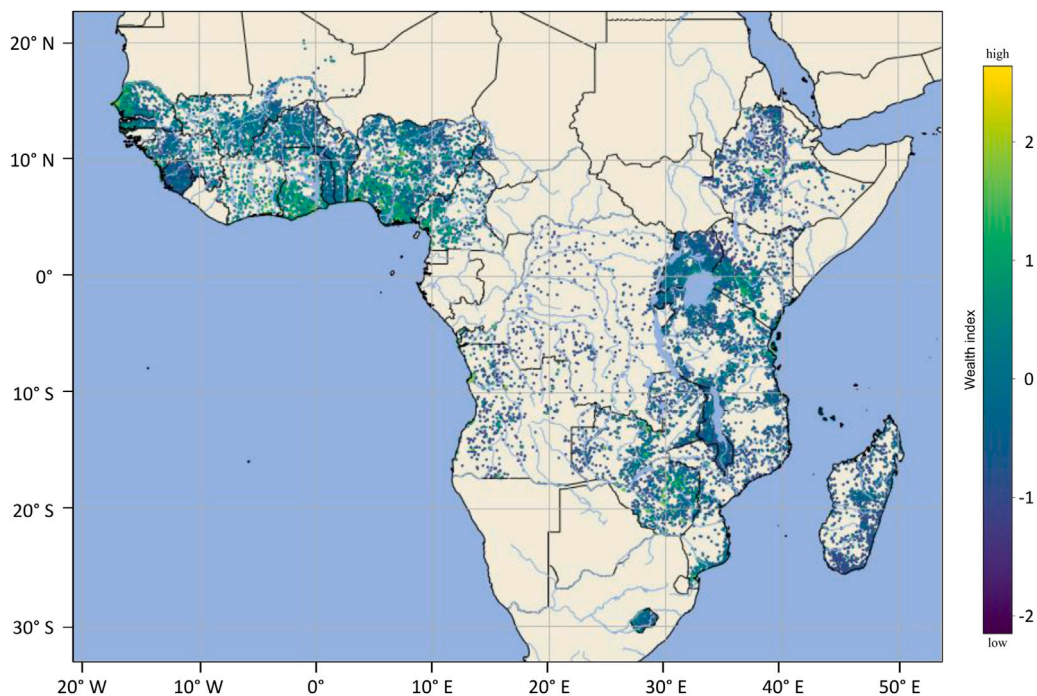
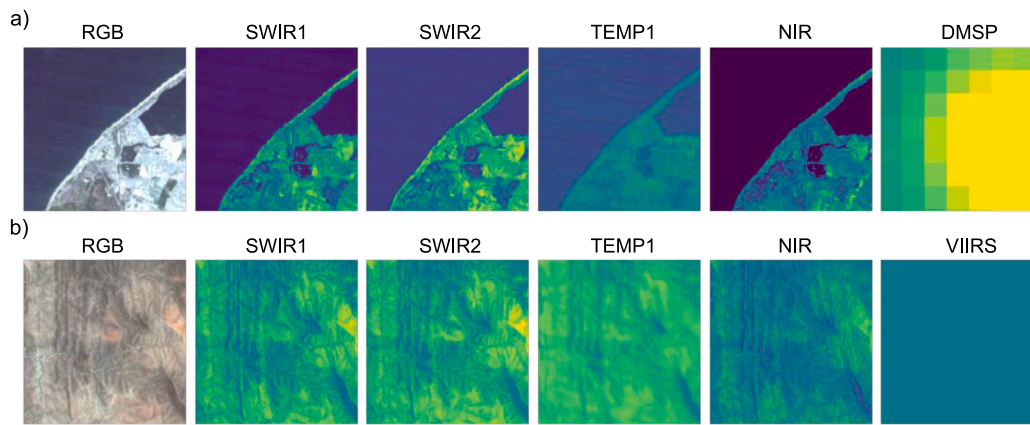


Fig. 2. The villages used to train the DL algorithm, were assigned their respective wealth index derived from DHS surveys (poorest in blue and richest in yellow). (For interpretation of the references to color in this figure legend, the reader is referred to the web version of this article.)



**Fig. 3.** Examples of Landsat Bands (RGB, SWIR1, SWIR2, TEMP1, NIR) and DMSP or VIIRS bands for two regions: (a) a region of Angola with a wealth index of 2.76 for 2011 (lat:  $-12.350$ , long:  $13.534$ ), and (b) a region of Kenya with a wealth index of  $-1.31$  for 2014 (lat:  $1.179$ , long:  $37.148$ ).

**Table 1**

Remote sensing satellites/sensor and products used in the project.

Type	Satellite/Sensor	Product
Daytime	Landsat 5 (1984–2013)	LANDSAT/LT05/C01/T1_SR
	Landsat 7 (1999–2022)	LANDSAT/LE07/C01/T1_SR
	Landsat 8 (2013–)	LANDSAT/LC08/C01/T1_SR
Nightlight	DMSP (Year $\leq 2011$ )	DMSP-OLS/CALIBRATED_LIGHTS_V4
	VIIRS (Year $\geq 2012$ )	VIIRS/DNB/MONTHLY_V1/VCMSLCFG

In the second phase, we downloaded satellite images based on the geographic coordinates of each village Fig. 3 to analyze images within  $\sim 6 \times 6$  km of the coordinates of the center of each village. Both MS and NL images were processed in, and exported from, Google Earth Engine with 3 years composition, and center-cropped to  $224 \times 224$  pixels (as pixels have a resolution of 30 m). Various daytime and night light satellite images were used (Landsat 5/7/8) [27], (Defense Meteorological Satellite Program (DMSP) [28]) and the Visible Infrared Imaging Radiometer Suite (VIIRS) [29]) (Table 1)

Information from all Landsat bands was used in the training, as well as that from the nightlight images. The Landsat bands consist of Red, Green, and Blue (RGB), Short-Wave Infrared 1 (SWIR1), Short-Wave Infrared 2 (SWIR2), Thermal Infrared 1 (TEMP1), and Near-Infrared (NIR). Examples of these bands are shown for two regions in Fig. 3, (a) for an area of high wealth index (2.76 in Angola in 2011) and (b) with a low wealth index ( $-1.31$  in Kenya in 2014). Satellite images from Landsat, DMSP, and VIIRS can all offer insights into a region's wealth index. For instance, areas with high wealth indices tend to have more vegetation and urban development.

## 2.2. Data split

The village wealth index dataset was split into five folds for the cross-validation. The CNN model was trained on 3-folds, validated on a 4th, and tested on a 5th. To prevent satellite image overlap between villages, we used two approaches: Out-Of-Country (OOC) and In-Country configurations. In the former, entire countries were allocated to a single split, whereas the latter allowed several clusters from the same country to be assigned to different splits.

## 2.3. CNN based-method

In DeepWealth, two separate CNNs based on the ResNet-18 architecture were trained on Landsat and NL imagery, respectively. The two-branch CNN used by DeepWealth was proposed by [13]. The final fully connected layers of both models were then fused. The ResNet-18

architecture, with a modified first convolutional layer, was used as a pre-trained model to take into account the multi-band of MS images.

Several configurations were tested (ResNet-18 MS+NL, ResNet-18 MS, ResNet-18 NL, ResNet-18 RGB). All the experiments used Python 3.7 with TensorFlow r1.15, and R 3.6. CNN models were trained with an Adam optimizer and a mean squared-error loss function. A batch size of 64 was employed, and the learning rate decayed by a factor of 0.96 after each epoch. The models were trained for 150 epochs for In-Country and for 200 epochs for OOC. The performance of the CNN model was tested on the testing set using the following configurations: ResNet-18 (MS+NL), ResNet-18 (MS), ResNet-18 (NL), ResNet-18 (RGB), and ResNet-18 (RGB+NL). The performance of the models for both approaches (OOC and In-Country) were very similar, the best fit being ResNet-18 (MS + NL) (Table 2).

## 3. Illustrative examples

Three case studies were used to evaluate DeepWealth. The first case study involved spatio-temporal mapping of the wealth index in Madagascar. Similarly, the second and third case study aims to show the mapping of wealth index and to evaluate the correlation with local socioeconomic data in Vale do Ribeira (Brazil), and Kita-Tōhoku region (Japan). It is important to emphasize that these three case studies are conducted independently, and are not aimed to make comparison between them.

### 3.1. Madagascar case study

As detailed in Section 2.1, DeepWealth was trained using data from 24 countries, including Madagascar. This case study aims to show how users can ingest new country data for training purposes, either from scratch or transfer learning. Madagascar, one of the world's poorest countries, has a significant percentage of its population living in extreme poverty. For training, we used the ground truth from Madagascar, encompassing 1509 surveyed villages over five years (1997, 2008, 2011, 2013 and 2016). Particularly, the performance evaluation for Madagascar yielded  $R^2 = 0.73$  for the ResNet-18 (MS + NL). The trained CNN model contains data from 24 countries, including Madagascar.

DeepWealth was used to map the wealth index in Madagascar at a fine scale. The resulting maps are presented in Fig. 4 at a resolution of  $\sim 6 \times 6$  km. The spatio-temporal mapping of wealth index in Madagascar from 1996 to 2020 suggests that the poorest populations are located in rural areas, in the southeast, and in coastal areas of the southwest. The poverty rate has decreased slightly over the past few years, but remains high, with over 70% of the population living below the poverty line. The estimated wealth index ranged from  $-1$  (poorest) to  $1.5$  (richest), corresponding to the minimum and maximum values found for Madagascar.



**Table 2**  
The coefficient of determination  $R^2$  for different CNN configurations.

	Resnet-18 MS+NL	Resnet-18 MS	Resnet-18 NL	Resnet-18 RGB	Resnet-18 RGB+NL
In-Country	0.691	0.66	0.66	0.60	0.67
OOC	0.67	0.61	0.62	0.60	0.66

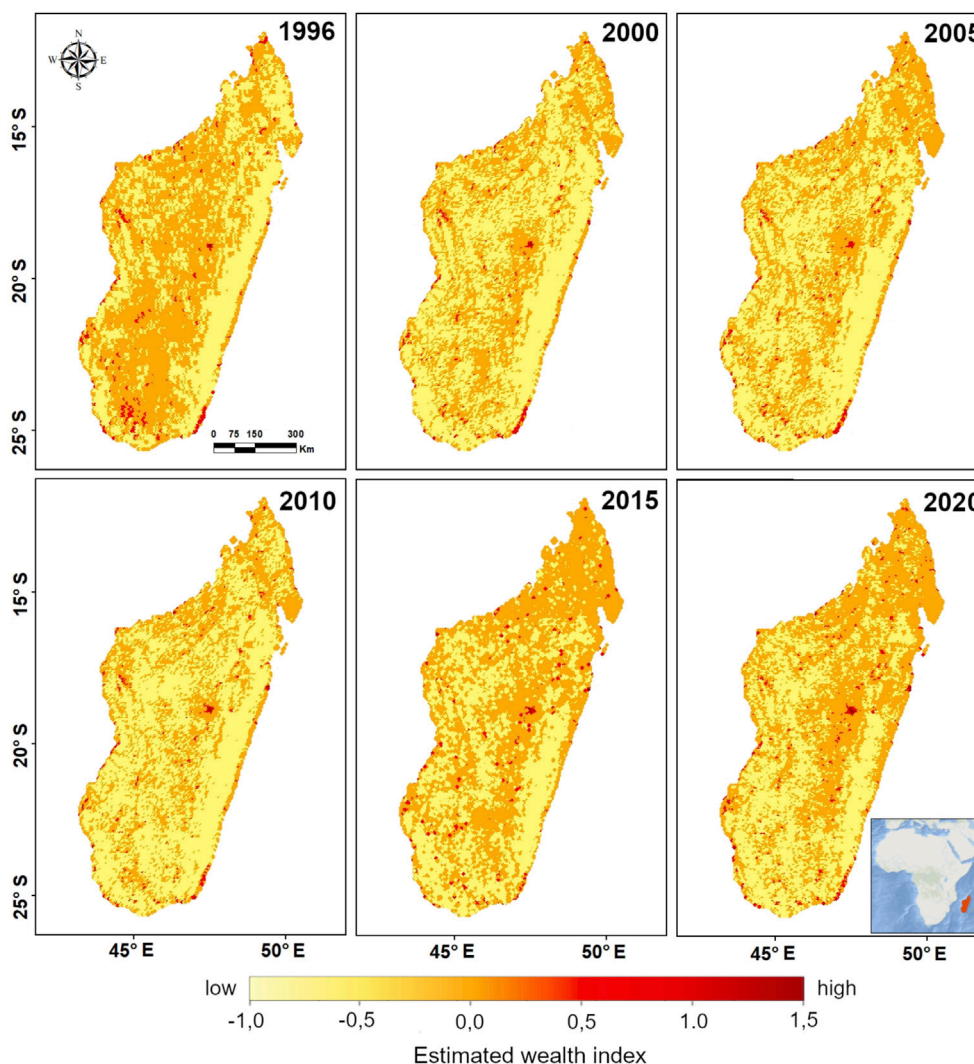


**Fig. 4.** Mapping of wealth index estimations in Madagascar from 1996 to 2020.

### 3.2. Vale do Ribeira, Brazil case study

The training checkpoints generated in DeepWealth were used to estimate a wealth index in a Brazilian scenario, specifically in the Vale do Ribeira region (VR). This was chosen because of data accessibility and the ecological and economic significance of the area. VR is located in the southern region of Brazil, encompassing the states of Paraná and São Paulo. With a total area 28,306 km<sup>2</sup>, it comprises 30 municipalities and contains 61% of Brazil’s remaining Atlantic forest, declared a UNESCO Natural Heritage of Humanity in 1999. To validate our estimations, we initially considered DHS data. However, it only covered Brazil for 1986, 1991, and 1996, lacking both recent data and geospatial information. Since this limited time frame did not align with available satellite imagery, we used the Human Development Index (HDI) at census sector level, which was derived from prior research [17], which relied on data from the Brazilian Institute of Geography and Statistics (IBGE) census surveys for their calculation.

Correlations were computed between the estimated wealth index values and the Brazilian’s HDI. In the cited work [17], the income

indicator was computed using variables from the Brazilian Institute of Geography and Statistics (IBGE) census 2010 survey. For this reason, we considered the 880 census sectors that have HDI available according to Brazilian census surveys of 2010. To compute the estimations, we used MS imagery only to estimate well-being. We made wealth index estimations on the VR region for the years 2010, 2015 and 2020 (Fig. 5) using the same shapefile and HDI dataset generated by [17]. Areas with high estimated indices (depicted in red) predominantly align with the urban areas within the region, which can be seen to increase slightly over the years.

We computed the Pearson correlation coefficient ( $r$ ) between the wealth index estimation obtained using DeepWealth and the real HDI indices, with a specific focus on its income dimension based on data from the 2010 Census Survey, the most recent available. We employed the dataset generated using the methodology by Machicao et al. [17] for the calculation of HDI indices. While it is important to acknowledge that the indices are not perfectly congruent, they do share analogous characteristics in evaluating the well-being of the population. Our

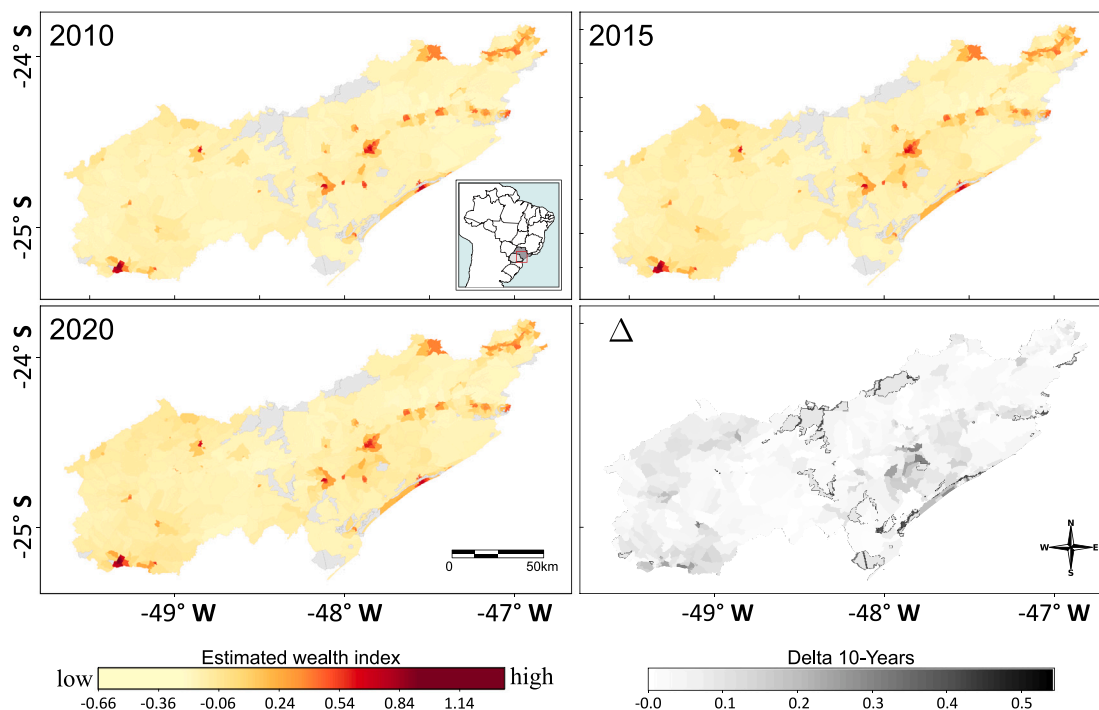


Fig. 5. Spatio-temporal mapping of wealth index estimations in Vale do Ribeira (southeast of Brazil) from 2010 to 2020 at census tract level. The bottom-right corner map illustrates the absolute difference ( $\Delta$ ) in estimated values between 2010 and 2020.

analysis produced a Pearson correlation coefficient,  $r = 0.53$  (Supplementary Table S1). As expected, this correlation is slightly less than the  $r = 0.69$  performance achieved by the DeepWealth model against DHS in the training phase with ResNet-18 MS+NL.

### 3.3. Kita-Tōhoku, Japan, case study

For the third case study we focused on the Kita-Tōhoku region, the northernmost part of Honshū Island, in Japan. This region spans 36,558 km<sup>2</sup> and includes the Aomori, Akita, and Iwate prefectures. The area is characterized by a rugged coastline, Ōu Mountains, and forests covering 72% of the land. We selected a sample of 15 municipalities (Shichinohe-machi, Takko-machi, Shingo-mura, Shizukuishi-machi, Kosaka-machi, Yokohama-machi, Ōma-machi, Higashidori-mura, Kazamaura-mura, Sai-mura, Kanegasaki-machi, Ōtsuchi-machi, Fudai-mura, Happo-machi, and Ugo-machi), having a total of 411 city/rural blocks, as the principal unit for disseminating small area statistics.

We estimated the wealth index for the period of years from 2000 to 2022 using NL imagery as input for the training checkpoints of the DeepWealth model (Fig. 6).

To validate these estimates, we conducted a correlation analysis using local economic variables at the municipality level (Supplementary Table S1). In Japan, where DHS data was unavailable, we relied on data from the Ministry of Internal Affairs and Communications for Taxable Income per Taxpayer (TXI) and the United Nations Development Programme for HDI income. We considered data from TXI over two decades, as well as HDI income over a 5-year period, as presented in Table S1. Pearson correlation coefficients were computed for both TXI ( $r = 0.53$ ) and HDI income ( $r = 0.64$ ) with the Deep Wealth estimated values, indicating moderate to strong associations. Notably, these results closely align with those obtained in the Brazilian case study, demonstrating consistency in performance.

## 4. Impact and conclusions

The combination of DL models and extensive EO databases has been gaining popularity for estimating socioeconomic indicators. This

combination demonstrates significant promise in providing accurate and actionable insights on the economic and social activities of various levels, along with supporting local governments, nonprofit organizations, and businesses to make informed decisions. Such insights are advantageous in tackling issues related to well-being reduction, disaster response, and sustainable development. Combining DL with EO data holds a strong potential to develop innovative and integrated solutions to address critical global challenges. Expanding from the work of [13], we have developed a comprehensive open-source framework capable of estimating well-being using satellite images that can be utilized by people with good knowledge of Python and R. Our approach combines data preprocessing techniques with state-of-the-art DL algorithms to extract relevant features and make accurate estimations.

DeepWealth has been shown to be generalizable across various regions and valuable to implement in a range of applications, and can provide granular wealth estimates at a high spatial resolution. As proof of concept, we showed that in Madagascar, the framework can be used to assess patterns of changes in the wealth index at the scale of the country. In Brazil, the framework can be used to analyze the impact of urbanization and population growth on natural resources such as forests and water, for instance. In Japan, the framework can be applied to study the socioeconomic impact of protected areas on touristic and non-touristic areas, to improve resource allocation and conservation strategies, for instance. Overall, DeepWealth has shown improved performance and can be useful for policymakers, more specifically, for spatio-temporal wealth index mapping, so that alleviation efforts and aid organizations in targeting their interventions. To facilitate fair comparisons among these case studies, further efforts are required to align the ground truth data and indices. However, it should be noted that these cases are for illustrative purposes regarding spatio-temporal mapping and should not be directly compared, as they represent independent cases.

DeepWealth was designed to facilitate replication and reproducibility in a variety of academic fields. It serves as a multi-disciplinary tool for users to ensure their research can be easily duplicated and verified by others. With its ability to generate consistent results, the platform

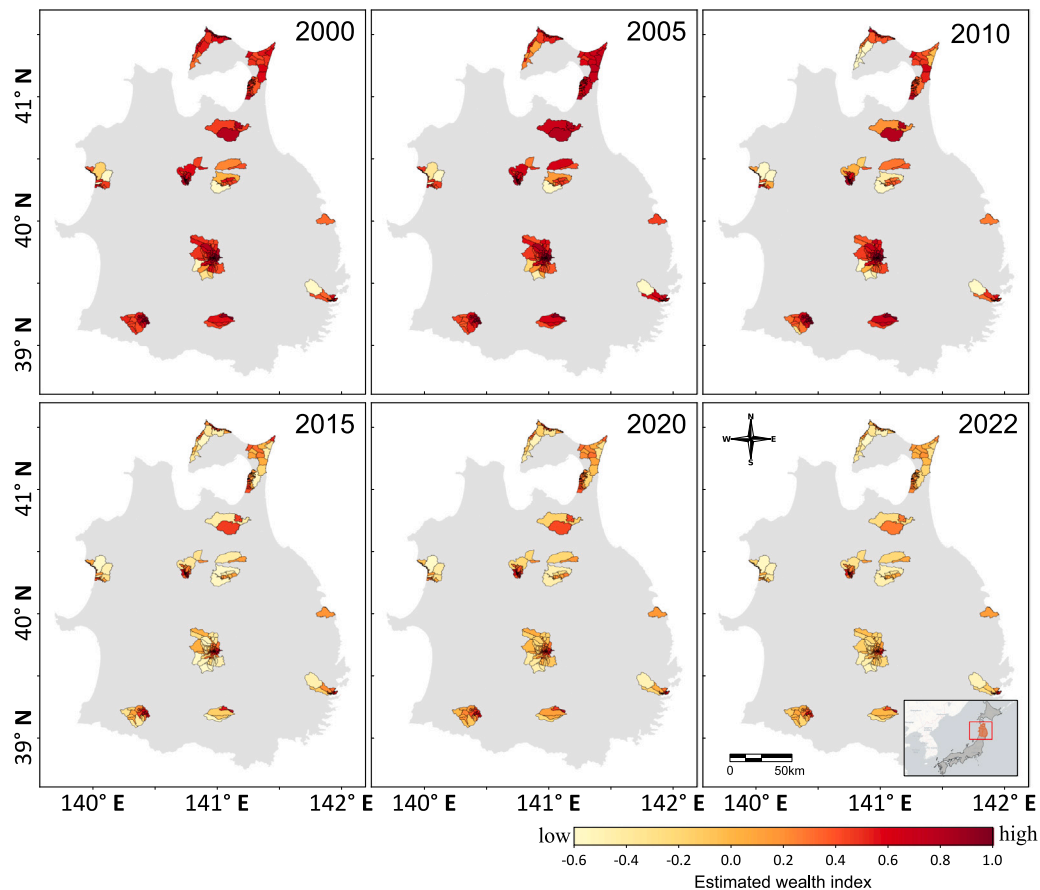


Fig. 6. Spatio-temporal mapping of wealth index estimations for some sample years in 15 municipalities from the Kita-Tōhoku region.

offers researchers an efficient way to manage data, collaborate with colleagues, and contribute to their respective fields. Overall, DeepWealth aims to support scientific rigor, transparency, and accountability across academic communities.

The three parts of DeepWealth (Fig. 1) can be used for future development. For example, the R script (A) enables the construction of a wealth index for a specific country or region over a specified period. The second part (B) enables the replication and reproduction of deep learning models in other areas and allows the incorporation of other indices such as health or water quality. The third part (C) is designed to use trained checkpoints to estimate the wealth index, offering a convenient and efficient way to generate novel estimations. A future direction could be to incorporate more satellite image products in DeepWealth, such as Sentinel-2, to enhance the estimation performance. This would not only increase the spatial resolution and accuracy of the predictions but also provide a more comprehensive understanding of the relationships between the various socioeconomic indicators and environmental factors. Additionally, integrating multi-task learning techniques would allow us to leverage correlated indices, such as health, water, and education, to improve the overall performance of the wealth index estimation.

#### CRediT authorship contribution statement

**Ali Ben Abbes:** Writing – review & editing, Writing – original draft, Visualization, Validation, Software, Methodology, Investigation, Formal analysis, Data curation, Conceptualization. **Jeaneth Machicao:** Writing – review & editing, Writing – original draft, Visualization, Validation, Software, Methodology, Investigation, Formal analysis, Data curation. **Pedro L.P. Corrêa:** Writing – review & editing, Writing –

original draft, Resources, Funding acquisition. **Alison Specht:** Writing – review & editing, Writing – original draft, Funding acquisition. **Rodolphe Devillers:** Writing – review & editing. **Jean P. Ometto:** Writing – review & editing. **Yasuhisa Kondo:** Writing – review & editing, Data curation. **David Mouillot:** Resources, Funding acquisition, Conceptualization.

#### Declaration of competing interest

The authors declare that they have no known competing financial interests or personal relationships that could have appeared to influence the work reported in this paper.

#### Data availability

A changelog of the source code can be found at Supplementary Material. Brazil: The HDI-income data for Vale do Ribeira was sourced from precalculated values reported by Machicao et al. [17] and presented in Supplementary Table S1. Japan: HDI-income and Taxable Income per taxpayer data for Japan were retrieved from United Nations Development Programme and the Ministry of Internal Affairs and Communications, respectively. The compiled results are included in Supplementary Table S2. The generated checkpoints of the trained model can be found in [30] (currently under embargo).

#### Acknowledgments

This project was conducted as part of the PARSEC project, funded under a Belmont Forum Collaborative Research Action (CRA) on Science-Driven e-Infrastructures Innovation (SEI), with funding from

the French ANR (grant number ANR-18-BELM-0002), the Japan Science and Technology Agency (JST: grant number 21-191029671), the National Science Foundation (NSF) of the USA (grant number 1929464), and the São Paulo Research Foundation (FAPESP: grant number 2018/24017-3), with support from the synthesis center CESAB of the French Foundation for Research on Biodiversity (FRB). ABA conducted the first part of the work while a postdoc at the CESAB-FRB working with staff of the Laboratory of Computer Science, Robotics and Microelectronics of Montpellier (LIRMM), and subsequently with funding from the University of São Paulo (grant 2022/14429-8). J.M. and JPO are grateful for the support from FAPESP (grant numbers 2020/03514-9 and 2017/22269-2, respectively). The authors thank Christopher Yeh from Computing and Mathematical Sciences (CMS) at Caltech, USA, for his generous assistance in addressing inquiries related to his previous work. The authors also thank Satoko Suetsugu (RIHN) for her help providing socioeconomic datasets and checking the manuscript. Special appreciation is also extended to Margaret O'Brien from the University of California, Santa Barbara (UCSB) and Shelley Stall from the American Geophysical Union (AGU) for their invaluable advice and support.

## Appendix A. Supplementary data

Supplementary material related to this article can be found online at <https://doi.org/10.1016/j.softx.2024.101785>.

## References

- [1] Arora NK, Mishra I. United Nations Sustainable Development Goals 2030 and environmental sustainability: race against time. *Environ Sustain* 2019;2(4):339–42.
- [2] Allen C, Smith M, Rabiee M, Dahmm H. A review of scientific advancements in datasets derived from big data for monitoring the sustainable development goals. *Sustain Sci* 2021;16(5):1701–16.
- [3] Persello C, Wegner JD, Hänsch R, Tuia D, Ghamisi P, Koeva M, et al. Deep learning and earth observation to support the sustainable development goals: Current approaches, open challenges, and future opportunities. *IEEE Geosci Remote Sens Mag* 2022;10(2):172–200.
- [4] Anderson K, Ryan B, Sonntag W, Kavvada A, Friedl L. Earth observation in service of the 2030 Agenda for Sustainable Development. *Geo-spat Inf Sci* 2017;20(2):77–96.
- [5] Paganini M, Petiteville I, Ward S, Dyke G, Steventon M, Harry J, et al. Satellite earth observations in support of the sustainable development goals. In: *The CEOS earth observation handbook*. Earth Observation Graphic Bureau (ESA) Venice, Italy; 2018.
- [6] Benhammou Y, Alcaraz-Segura D, Guirado E, Khaldi R, Achchab B, Herrera F, et al. Sentinel2GlobalLULC: A Sentinel-2 RGB image tile dataset for global land use/cover mapping with deep learning. *Sci Data* 2022;9(1):681.
- [7] Xie F, Zhou J, Lee JW, Tan M, Li S, Rajnithern LS, et al. Benchmarking emergency department prediction models with machine learning and public electronic health records. *Sci Data* 2022;9(1):658.
- [8] Han Q, Zeng Y, Zhang L, Wang C, Prikaziuk E, Niu Z, et al. Global long term daily 1 km surface soil moisture dataset with physics informed machine learning. *Sci Data* 2023;10(1):101.
- [9] Chen F-XR, Lin C-Y, Siao H-Y, Jian C-Y, Yang Y-C, Lin C-L. Deep learning based atomic defect detection framework for two-dimensional materials. *Sci Data* 2023;10(1):91.
- [10] Reichstein M, Camps-Valls G, Stevens B, Jung M, Denzler J, Carvalhais N, et al. Deep learning and process understanding for data-driven earth system science. *Nature* 2019;566(7743):195–204.
- [11] LeCun Y, Bengio Y, Hinton G. Deep learning. *Nature* 2015;521(7553):436–44.
- [12] Goodfellow I, Bengio Y, Courville A. Deep learning. MIT Press; 2016.
- [13] Yeh C, Perez A, Driscoll A, Azzari G, Tang Z, Lobell D, et al. Using publicly available satellite imagery and deep learning to understand economic well-being in Africa. *Nat Commun* 2020;11(1):2583.
- [14] Machicao J, Ben Abbes A, Meneguzzi L, Corrêa P, Specht A, David R, et al. Mitigation strategies to improve reproducibility of poverty estimations from remote sensing images using deep learning. *Earth Space Sci* 2022;9(8). e2022EA002379.
- [15] Jean N, Burke M, Xie M, Davis WM, Lobell DB, Ermon S. Combining satellite imagery and machine learning to predict poverty. *Science* 2016;353(6301):790–4.
- [16] Burke M, Driscoll A, Lobell DB, Ermon S. Using satellite imagery to understand and promote sustainable development. *Science* 2021;371(6535):eabe8628.
- [17] Machicao J, Specht A, Vellenich D, Meneguzzi L, David R, Stall S, et al. A deep-learning method for the prediction of socio-economic indicators from street-view imagery using a case study from Brazil. *Data Sci J* 2022;21.
- [18] Wölk F, Yuan T, Kis-Katos K, Fu X. A temporal-spatial analysis on the socioeconomic development of rural villages in Thailand and Vietnam based on satellite image data. *Comput Commun* 2023;203:146–62.
- [19] Yin H, Zhou K. Performance evaluation of China's photovoltaic poverty alleviation project using machine learning and satellite images. *Util Policy* 2022;76:101378.
- [20] Castro DA, Álvarez MA. Predicting socioeconomic indicators using transfer learning on imagery data: an application in Brazil. *Geojournal* 2023;88(1):1081–102.
- [21] Balas VE, Roy SS, Sharma D, Samui P. *Handbook of deep learning applications*. Springer Cham; 2019.
- [22] Suel E, Bhatt S, Brauer M, Flaxman S, Ezzati M. Multimodal deep learning from satellite and street-level imagery for measuring income, overcrowding, and environmental deprivation in urban areas. *Remote Sens Environ* 2021;257:112339.
- [23] Wilkinson MD, Dumontier M, Aalbersberg IJ, Appleton G, Axton M, Baak A, et al. The FAIR guiding principles for scientific data management and stewardship. *Sci Data* 2016;3(1).
- [24] Watson OJ, FitzJohn R, Eaton JW. RDHS: an R package to interact with the Demographic and Health Surveys (DHS) Program datasets. *Wellcome Open Res* 2019;4(103):103.
- [25] Filmer D, Scott K. Assessing asset indices. *Demography* 2012;49(1):359–92.
- [26] Alkire S, Roche JM, Ballon P, Foster J, Santos ME, Seth S. *Multidimensional poverty measurement and analysis*. USA: Oxford University Press; 2015.
- [27] Wulder MA, Loveland TR, Roy DP, Crawford CJ, Masek JG, et al. Current status of Landsat program, science, and applications. *Remote Sens Environ* 2019;225:127–47.
- [28] Hsu F-C, Baugh KE, Ghosh T, Zhizhin M, Elvidge CD. DMSP-OLS radiance calibrated nighttime lights time series with intercalibration. *Remote Sens* 2015;7(2):1855–76.
- [29] Elvidge CD, Baugh K, Zhizhin M, Hsu FC, Ghosh T. VIIRS night-time lights. *Int J Remote Sens* 2017;38(21):5860–79.
- [30] Ben Abbes A, Machicao J, Corrêa PLP, Specht A, Devillers R, Ometto J, et al. DeepWealth: Checkpoints from the trained deep learning model to use satellite images for poverty estimation [data set]. 2024, <http://dx.doi.org/10.5281/zenodo.10575637>, Zenodo.